



## Magnetohydrodynamic Heat and Mass Transfer in Cu–H<sub>2</sub>O and Al<sub>2</sub>O<sub>3</sub>–H<sub>2</sub>O Nanofluids over a Permeable Extended Surface with Chemical Reactions and Thermal Radiation

Veera Reddy. Karnati<sup>1\*</sup>, Akkenapalli Padma<sup>2</sup>, Vijaya Kumar. D<sup>3</sup>, B. Lavanya<sup>4</sup>, S. Gouthamsri<sup>5</sup>, Pathuri Bindu<sup>6</sup>, G. Venkata Ramana Reddy<sup>7</sup>

<sup>1,\*</sup>Department of Mathematics, Guru Nanak Institutions Technical Campus, Ibrahimpatnam, R.R.Dist, Telangana, India-501506.

<sup>2</sup>Department of Mathematics, Chaitanya Bharathi Institute of Technology, Gandipet, Hyderabad, Telangana, India-500075.

<sup>3</sup>Department of Applied Mathematics, Lakireddy Bali Reddy College of Engineering, Mylavaram, Andhra Pradesh, India-521230.

<sup>4</sup>Department of Basic Sciences and Humanities, Vignan's Nirula Institute of Technology and Science for Women, Guntur, Andhra Pradesh, India-522009

<sup>5</sup>Department of Chemistry, Aditya Institute of Technology and Management, Tekkali, AP, India-532201.

<sup>6</sup>Department of Mathematics, Koneru Lakshmaiah Education Foundation, Vaddeswaram, Guntur (Dt), AP, India-522302.

<sup>7</sup>Department of IRD, Koneru Lakshmaiah Education Foundation, Vaddeswaram, Guntur, India-522302.

Email: veerareddymcmed@gmail.com, padma\_maths@cbit.ac.in, vijaymym1@gmail.com, lavanyabandaru85@gmail.com,

bindupathuri@kluniversity.in, gvrr1976@kluniversity.in.

Corresponding Email: veerareddymcmed@gmail.com

**Abstract:** The dynamics of mass transport and convective heat in a magneto hydrodynamic nanofluid passing through a permeable medium on top of an extended surface while being subjected to a magnetic field are investigated in this publication. Chemical processes, thermal radiation, viscosity dissipation, and heat creation are all included in the extensive analytical model. We discuss in detail some of the governing properties, such as heat generation, thermal radiation, magnetic fields, chemical processes, porosity, and viscous dissipation. Additionally, the volumetric distribution of nanoparticles at the boundary interface is proposed to be controllable. This investigation focuses on two distinct types of nanofluids: Cu-H<sub>2</sub>O and Al<sub>2</sub>O<sub>3</sub>-H<sub>2</sub>O. The problem is theoretically framed in terms of a system of nonlinear differential equations. These are then solved numerically by combining the shooting method with the fourth-order Runge-Kutta methodology. Our results show good agreement with those that have been previously published in the academic literature.

**Keywords:** Hybrid nanofluids; MHD; Porous media; Thermal radiation; Skin-friction.



## **1. Introduction**

The examination of Nano fluids has gotten a considerable sum of consideration in modern scholastic talk. Usually due to the reality that nanofluids have made strides warm properties in differentiate to customary liquids. Nanofluids are a novel category of liquids that are characterised by the nearness of nanoparticles that are suspended inside a substrate liquid. As a result of the extraordinary warm exchange capabilities that they have, they have risen as a potential choice for a huge assortment of mechanical applications. The marvels of boundary layer stream and warm exchange over extended surfaces are basic components of an assortment of building forms. These operations incorporate the expulsion of polymer sheets, strengthening, gem arrangement forms, metal turning, and hot rolling. It was Crane [1] who played a noteworthy part within the starting stages of the examination of stream flow past a extending plate. Hence, an expansive number of analysts have examined the stream and warm exchange characteristics of an assortment of liquids over extended surfaces. The stream of a nanofluid by means of a extended sheet was examined by Khan and Pop [2], who carried out an examination into the boundary layer stream. With an emphasis on the consequences of thermal diffusion, Abd El-Aziz examined the combined heat and mass transfer processes in this work [3] and diffusion thermo when a hydromagnetic fluid is free to move across a porous stretched surface in three dimensions while taking thermal radiation into account. An investigation by Hady and colleagues [4] evaluated the effects of radiation on the viscous flow of a nanofluid and the heat exchange across a nonlinearly stretched sheet. Bachok et al. [5] examined the unstable boundary-layer flow and heat transmission characteristics of a nanofluid spanning a permeable stretching/shrinking sheet. In their consider, Rohni and colleagues [6] used Buongiorno's show to examine the stream and warm exchange characteristics that happened over an unsteady contracting sheet that was subjected to suction in a nanofluid. In arrange to clarify the convective transport forms that take put in nanofluids, Buongiorno [7] proposed a show that comprises of two components. The impact of heat and mass transfer on a magnetohydrodynamic (MHD) flows over an incline permeable plate while accounting for a chemical reaction was examined by Sandhya et al. [8]. A non-Darcy common convection administration was the subject of an examination by Murthy and Singh [9], who explored the suggestions of gooey scattering. Motsa [10] displayed an interesting ghostly unwinding method for the examination of closeness variable nonlinear boundary layer stream frameworks. This method was created especially for those frameworks. Gladys and Reddy [11] examined how a stream of non-Newtonian nanofluid moving across an accelerating vertical plate is affected by variations in thermal conductivity and consistency. Vijaya and Reddy [12] investigated the Casson liquid flow over a vertical permeable plate using magnetohydrodynamics while accounting for the effects of chemical reactions, radiation, and Soret (thermo-diffusion). A numerical examination into common convection was carried out by Oztop and AbuNada [13] inside rectangular walled in areas that were in part warmed and filled with nanofluids to explore the wonder. A demonstrate in which the thickness of concentrated suspensions and arrangements is taken into thought was created by Brinkman [14]. Maxwell Garnett [15] created a conceptual system that gives a clarification for the colouration marvels that are watched in metallic oxide coatings and glasses. The application of nanofluids for the reason of upgrading warm exchange in isolated streams that are experienced in backward-facing steps was examined by Abu-Nada [16]. Beneath the impact of a attractive field, Hamad [17] was able to get an expository arrangement for the common convection stream of a nanofluid over a sheet that was amplifying in a direct method. A think about conducted by Kameswaran and colleagues [18] looked into the hydromagnetic stream of nanofluids that happened as a result of a sheet that was either extended or contracted. The analysts took into consideration the impacts of thickness dissemination and chemical intuitive. The highlights of warm exchange that are associated with a persistent extended surface that's subject to fluctuating temperature conditions were explored by Grubka and Bobba [19]. Rafique et al. [20] shown improved performance under a range of slip and viscosity conditions in their thorough mathematical study of hybrid nanofluid flow under magneto hydrodynamic (MHD) effects. While studying thermal transport in single-phase nanofluid flow over radially stretched disks, Nisar et al. [21] shown that titanium dioxide



*Received: 16-09-2025*

*Revised: 05-10-2025*

*Accepted: 02-11-2025*

nanoparticles in a water base significantly improve heat transfer rates. The effect of oxytactic microorganisms was taken into consideration when Patil et al. [22] investigated the actions of magnetized bio-convective micropolar nanofluids moving across a wedge. Rawat et al. [23] investigated how non-uniform heat sources/sinks and nanoparticle aggregation influenced the flow properties of a titania-ethylene glycol nanofluid within a wedge-shaped region. An electrically conducting micropolar nanofluid passing through a wedge geometry was examined by Umavathi [24], taking into account the effects of ion and Hall currents, as well as internal heat generation and absorption. Veera [25] investigated the chemical and electromagnetic interactions within an unsteady magnetohydrodynamic (MHD) viscoelastic flow (Walter's B fluid) over vertical porous plates.

### Significance and objective

This study is important because it thoroughly examines how thermal radiation and Magnetohydrodynamic (MHD) hybrid nanofluid flow properties over porous stretching surfaces are influenced by chemical processes. The impact of magnetic fields, heat radiation, and velocity slip conditions are specifically examined in relation to a hybrid nanofluid made up of  $AlO_3$ -Cu nanoparticles suspended in water. Magnetohydrodynamics and thermal management gain important new insights from this work, which also presents a novel method for comprehending complex fluid dynamics. Industries including chemical engineering, biomedical engineering, and polymer processing can benefit from its practical implications.

The study addresses critical research gaps in the following areas:

- **Behavior under similar conditions:** Investigating hybrid nanofluids under analogous conditions enables the identification of distinct flow and thermal characteristics, directly impacting their practical applications.
- **Role of the stretching sheet and inclination:** The stretching surface influences material properties like thickness, strength, and flexibility. Additionally, inclination modifies convective behavior through buoyancy-gravity interaction, which is essential in biofluid mechanics, manufacturing, and aerospace systems.
- **Importance of thermal radiation:** Accurately modeling thermal radiation is vital in high-temperature environments such as those found in aerospace applications.
- **Function of porous media:** Porous substrates increase surface area and stabilize fluid flow, making them beneficial in cooling systems for automotive and aerospace applications.
- **Magnetic field effects on non-Newtonian fluids:** Understanding MHD behavior can drive innovations in nuclear reactor cooling systems and magnetic drug targeting technologies.
- **Soret effect:** This thermophoretic phenomenon describes mass diffusion in nanofluids and is critical for precise modeling of hybrid systems.
- **Hybrid nanofluids in heat transfer:** The use of  $Al_2O_3$ -Cu/water nanofluid enhances thermal conductivity, making it an ideal medium for modern cooling and heat exchange technologies.

The following research questions serve as the basis for our study:

- What is the behavior of various non-Newtonian hybrid nanofluids across an inclining Stretching surface?
- How does adding a stretching surface to the model affect things?



Received: 16-09-2025

Revised: 05-10-2025

Accepted: 02-11-2025

- How does the Soret effect, heat sources, and thermal radiation affect the temperature distribution of the flow?
- Nanoparticles have a variety of effects on fluid flow and heat transfer characteristics.

## 2. Mathematical Formulation

The following elements are considered in order to describe this study:

- The goal of this request is to better understand the improved mass and heat transfer of an incompressible nanofluid flowing steadily in two dimensions via a boundary layer over a permeable stretching sheet.
- The opening from which the sheet amplifies serves as the beginning point for the framework, which is situated at the beginning point.
- The x-axis is adjusted to line up with the continually stretching surface in this particular structural configuration.
- The perpendicular alignment of the y-axis to the surface plane of the sheet is what distinguishes it.
- In comparison to the attractive field that's connected from the exterior, it is considered that the attractive field that's delivered by the stream is nothing more than an unimportant sum.
- Furthermore, it is possible to claim that the attractive field that's created, at the side the electric field that's show exterior and the field that's delivered by charge partition, are of moderately little importance when compared to the attractive field that's forced from the exterior.
- In expansion, the impacts of chemical warming, nanoparticle agglomeration, and sedimentation have been intentionally cleared out of the investigation that's being displayed here.
- Copper nanoparticles and Al<sub>2</sub>O<sub>3</sub> nanoparticles are spoken to within the nanofluid that's being explored.
- Two distinct types of nanoparticles are combined to form this nanofluid from a basis that is primarily made of water.
- Since it is believed that the base liquid and the nanoparticles are in a heated concord, it is unlikely that any slip events will occur between the two distinct stages.
- Table 1 shows the properties linked to the nanofluid's thermophysical conduct.
- The overseeing boundary layer conditions that are pertinent to the nanofluid stream can be verbalized in dimensional shape by Gladys et al. [11].
- These conditions incorporate the progression, energy, velocity, and concentration areas, as well as the impacts of dissemination, radiation, heat source, and chemical responses.

The previously mentioned premises are essential for the definition of these conditions.

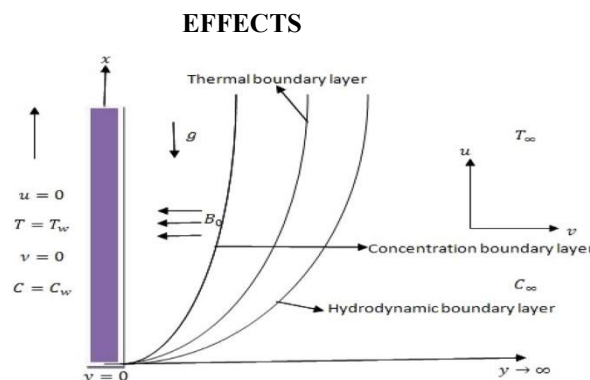


Fig. 1. Physical geometry.



$$u \frac{\partial u}{\partial x} + v \frac{\partial v}{\partial y} = 0, \quad (2.1)$$

$$u \frac{\partial u}{\partial x} + v \frac{\partial u}{\partial y} = \frac{\mu_{nf}}{\rho_{nf}} \left( 1 + \frac{1}{\beta} \right) \frac{\partial^2 u}{\partial y^2} - \left\{ \frac{\mu_{nf}}{\rho_{nf}} \frac{1}{K} + \frac{\sigma B_0^2}{\rho_{nf}} \right\} u \quad (2.2)$$

$$u \frac{\partial T}{\partial x} + v \frac{\partial T}{\partial y} = \alpha_{nf} \frac{\partial^2 T}{\partial y^2} + \frac{Q_0}{(\rho c_p)_{nf}} (T - T_\infty) + \frac{1}{(\rho c_p)_{nf}} \frac{16\sigma^* T_\infty^3}{3K^*} \frac{\partial^2 T}{\partial y^2} + \frac{\mu_{nf}}{(\rho c_p)_{nf}} \left( \frac{\partial u}{\partial y} \right)^2 \quad (2.3)$$

$$u \frac{\partial C}{\partial x} + v \frac{\partial C}{\partial y} = D_B \frac{\partial^2 C}{\partial y^2} + \frac{D_T}{T_\infty} \frac{\partial^2 T}{\partial y^2} - K_0 (C - C_\infty) \quad (2.4)$$

The following describes the boundary conditions for (1) to (4):

$$\begin{cases} u = ax, v = 0, T = T_w(x) = T_\infty + m \left( \frac{x}{\omega} \right)^2, C = C_w(x) = C_\infty + n \left( \frac{x}{\omega} \right)^2 & \text{at } y = 0 \\ u \rightarrow 0, T \rightarrow T_\infty, C \rightarrow C_\infty & \text{as } y \rightarrow \infty \end{cases} \quad (2.5)$$

The constants  $n, m$  and  $a$  are used here, with  $a > 0$  and  $w$  standing for the characteristic length. According to [12], the radiation heat flux,  $q_r$ , is as follows:

$$q_r = - \frac{4\sigma^*}{3K^*} \frac{\partial T^4}{\partial y}, \quad (2.6)$$

In this case,  $\sigma^*$  stands for the Stefan-Boltzmann constant, and  $K^*$  is the Rosseland mean absorption coefficient as determined by P. An expansion of the Taylor series is used to express the temperature fluctuation  $T^4$ . By expanding  $T^4$  around  $T_\infty$  and neglecting higher-order terms, the resulting expression is:

$$T^4 = 4T_\infty^3 - 3T_\infty^4. \quad (2.7)$$

Brinkman [14] provided the nanofluid's effective dynamic viscosity as

$$\mu_{nf} = \frac{\mu_f}{(1-\phi)^{2.5}}, \quad (2.8)$$

The dynamic viscosity of the base fluid is denoted by  $\mu_f$ , whereas  $\phi$  stands for the solid volume fraction of nanoparticles. Equations (1) through (4) use the Maxwell-Garnett model (see Maxwell Garnett [15]) to calculate the thermal capacitance and thermal conductivity of the nanofluid; however, the model is only applicable to spherical nanoparticles.

$$\begin{aligned} (\rho c_p)_{nf} &= (1-\phi)(\rho c_p)_f + \phi(\rho c_p)_s, \\ \rho_{nf} &= (1-\phi)\rho_f + \phi\rho_s, v_{nf} = \frac{\mu_{nf}}{\rho_{nf}}, \\ \alpha_{nf} &= \frac{k_{nf}}{(\rho c_p)_{nf}}, k_{nf} = k_f \left[ \frac{(k_s+k_f)-2\phi(k_f-k_s)}{(k_s+k_f)+\phi(k_f-k_s)} \right], \end{aligned} \quad (2.9)$$

where  $v_{nf}, \rho_{nf}, (\rho c_p)_{nf}, k_{nf}, k_f, k_s, \rho_s, (\rho c_p)_f, (\rho c_p)_s$ , electrical conductivity properties, the terms refer, in order, to the nanofluid's specific heat capacity, nanofluid's thermal conductivity, base fluid's thermal conductivity, solid constituents' thermal conductivity, density linked to the solid constituents, base fluid's heat capacity, and effective heat capacity resulting from nanoparticles.

When the stream function  $\psi(x,y)$  is introduced, the equation for continuity (2.1) is satisfied in the following way:



$$u = \frac{\partial \psi}{\partial y}, v = -\frac{\partial \psi}{\partial x} \quad (2.10)$$

Let's introduce the following non-dimensional variables:

$$\begin{aligned} \psi &= [av_f]^{1/2} x f(\eta), u = axf'(\eta), v = -(av_f)f(\eta), \\ \theta(\eta) &= \frac{T-T_\infty}{T_w-T_\infty}, \varphi(\eta) = \frac{C-C_\infty}{C_w-C_\infty}, \eta = \left[\frac{a}{v_f}\right]^{1/2} y \end{aligned} \quad (2.11)$$

$\theta(\eta)$  stands for the dimensionless temperature,  $f(\eta)$  for the dimensionless stream function,  $\theta(\eta)$  for the dimensionless concentration, and  $\eta$  for the similarity variable.

By combining equations (2.6) to (2.11) with the fundamental equations (2.2), (2.3), and (2.4), and incorporating the boundary conditions (2.5), we formulate the following two-point boundary value problem:

$$\left(1 + \frac{1}{\beta}\right) f'''' + \omega_1 [ff'' - f'^2 - \frac{1}{\omega_2} Mf'] - K_1 f' = 0, \quad (2.12)$$

$$\left(1 + \frac{4R}{3}\right) \theta'' + \omega_3 [f\theta' - 2f'\theta + Q\theta + \frac{E_c}{\omega_4} f''^2] = 0, \quad (2.13)$$

$$\varphi'' + Sc(f\varphi' - 2f'\varphi + Kr\varphi) + Sr\theta'' = 0. \quad (2.14)$$

subject to the boundary conditions

$$\begin{cases} f = 0, f' = 1, \theta = 1, \varphi = 1 & \text{at } \eta = 0 \text{ and} \\ f' \rightarrow 0, \theta \rightarrow 0, \varphi \rightarrow 0 & \text{as } \eta \rightarrow \infty. \end{cases} \quad (2.15)$$

The base fluid's kinetic viscosity and thermal diffusivity are crucial parameters are represented by  $\nu_f = \mu_f/\rho_f$  and  $\alpha_f = k_f/(\rho_f c_p)$ , respectively, Primes signify difference in relation to  $\eta$ . Other non-dimensional parameters that show up in equations (2.12) to (2.15) include the scaled chemical reaction parameter  $M, K_1, R, Pr, Q, E_c, Sc, Kr$ , the Soret and Prandtl numbers, heat generation parameters, Schmidt and Eckert numbers, additionally taken into account were the thermal radiation, magnetic, and porous medium parameters.

The mathematical definition of these parameters is

$$\begin{aligned} M &= \frac{\sigma B_0^2}{a\rho_f}, K_1 = \frac{v_f}{ak'}, R = \frac{4\sigma^* T_\infty^3}{k^* k_{nf}}, Sc = \frac{v_f}{D}, \\ Pr &= \frac{v_f(\rho c_p)_f}{k_f}, Q = \frac{Q_0}{a(\rho c_p)_{nf}}, Kr = \frac{K_0}{a}, \\ E_c &= \frac{u_w^2}{(T_w-T_\infty)(c_p)_f}, Sr = \frac{D_1(T_w-T_\infty)}{D(C_w-C_\infty)}. \end{aligned} \quad (2.16)$$

The volume fractions of nanoparticles,  $\phi_1$  and  $\phi_2$ , are

$$\begin{aligned} \omega_1 &= (1 - \phi)^{2.5} \left[ 1 - \phi + \phi \left( \frac{\rho_s}{\rho_f} \right) \right], \omega_2 = 1 - \phi + \phi \left( \frac{\rho_s}{\rho_f} \right), \\ \omega_3 &= 1 - \phi + \phi \left( \frac{\rho c_p}_s}{\rho c_p}_f \right), \omega_4 = (1 - \phi)^{2.5} \left[ 1 - \phi + \phi \left( \frac{\rho c_p}_s}{\rho c_p}_f \right) \right]. \end{aligned} \quad (2.17)$$



Received: 16-09-2025

Revised: 05-10-2025

Accepted: 02-11-2025

### 3. Coefficients of mass, heat and skin friction

The local Sherwood number,  $Sh_x$ , the regional Nusselt number  $Nu_x$ , and the skin's friction coefficient  $C_f$  are important from an engineering standpoint. These numbers describe the mass transfer, wall heat transfer, and surface drag rates, respectively.

At the surface of the wall, the shearing stress  $\tau_w$  is defined as

$$\tau_w = -\mu_{nf} \left( \frac{\partial u}{\partial y} \right)_{y=0} = -\frac{1}{(1-\phi)^{2.5}} \rho_f \sqrt{v_f a^3} x f''(0), \quad (3.1)$$

The viscosity coefficient is denoted as  $\mu_{nf}$ . The skin friction coefficient is calculated as:

$$C_{fx} = \frac{2\tau_w}{\rho_f U_w^2}, \quad (3.2)$$

Upon substituting equation (3.1) into (3.2), the result is:

$$0.5(1-\phi)^{2.5} C_{fx} = -Re_x^{-\frac{1}{2}} f''(0). \quad (3.3)$$

The following is a definition of the heat transfer rate over the wall's surface flux:

$$q_w = -k_{nf} \left( \frac{\partial T}{\partial y} \right)_{y=0} = -k_{nf} \frac{(T_w - T_\infty)}{x} \sqrt{\frac{U_w x}{v_f}} \theta'(0), \quad (3.4)$$

where  $k_{nf}$  represents the nanofluid's thermal conductivity. To define the local Nusselt number, one way is

$$Nu_x = \frac{x q_w}{k_f (T_w - T_\infty)}. \quad (3.5)$$

To calculate the rate of heat transfer through dimensionless walls, we substitute equation (3.4) into equation (3.5), which yields:

$$\left( \frac{k_f}{k_{nf}} \right) Nu_x = -Re_x^{0.5} \theta'(0). \quad (3.6)$$

The following is a description of the volume of fluxes at the wall surface:

$$q_m = -D \left( \frac{\partial C}{\partial y} \right)_{y=0} = -DQ \left( \frac{x}{\omega} \right)^2 \sqrt{\frac{a}{v_f}} \varphi'(0), \quad (3.7)$$

The Sherwood number for the area is obtained as:

$$Sh_x = \frac{x q_m}{D(C_w - C_\infty)}. \quad (3.8)$$

By using equations (3.7) and (3.8), the dimensionless wall transfer rate of mass can be calculated as follows:

$$Sh_x = -Re_x^{\frac{1}{2}} \varphi'(0) \quad (3.9)$$

$Re_x$ , the local Reynolds number, is defined as

$$Re_x = \frac{x u_w}{v_f}$$



#### 4. Method of solution

The mathematical expressions that are symbolized by the numbers (2.12) to (2.14) display a significant degree of non-linearity, which has the effect of making the process of deriving explicit solutions more difficult. Since this is the case, the resolutions of these mathematical constructs, together with the boundary conditions discussed in (2.15), the shooting method and the fourth-order Runge-Kutta approach were used to produce numerical solutions.

#### 5. Results and Discussion

An analytical solution to the nonlinear boundary value problem defined by equations (2.12) – (2.14), along with the boundary conditions outlined in (2.15) and (2.16), is not feasible due to its complexity. Thus, the shooting approach and the fourth-order Runge-Kutta technique are combined to solve the issue numerically. These numerical methods are primarily used for water-based nanofluids, such as Cu-water, under the assumption that the Prandtl number is constant and that water is the base fluid. Table 1 presents the thermophysical characteristics of the nanofluids utilized in the simulations. The velocity, temperature, and concentration profiles were determined using extensive numerical calculations. By combining the shooting methodology with the fourth-order Runge-Kutta method, the issue is solved numerically. These numerical techniques are specifically applied to Cu-water and other water-based nanofluids, thinking that the Prandtl number is constant and that water is the base fluid. The thermophysical characteristics of the simulations' nanofluids are shown in Table 1. Temperature, concentration, and velocity profiles were established by means of rigorous numerical simulations.

Figures 2 through 11 provide a detailed illustration of how various physical parameters affect the dynamic properties of Cu-water and  $AlO_3$ -water nanofluids. More precisely, Figure 2 shows how the velocity profile of both nanofluids is affected by the magnetic parameter ( $M$ ). Both Cu-water and  $AlO_3$ -water nanofluids exhibit a discernible decrease in velocity as  $M$  increases. The Lorentz force, which develops when a magnetic field is applied perpendicular to an electrically conductive fluid, is mostly to blame for this slowing. This force prevents the fluid from moving freely within the boundary layer by acting as a resistive mechanism. Consequently, the temperature of the fluid and the concentration of the solute both rise concurrently with this decrease in velocity.

Figure 3 examines the connection between the velocity of the nanofluids and the permeability parameter  $K_1$  of the porous material. Both Cu-water and  $AlO_3$ -water nanofluids see a drop in velocity when  $K_1$  increases. As the graph makes evident, the  $AlO_3$ -water nanofluid continuously displays a higher velocity profile than the Cu-water variety.

Figures 4 through 6 analyze how temperatures, velocity, and concentration of solute are affected by the volume and percentage of nanoparticles in both nanofluids. Clearly, the velocity of the Cu-water nanofluid decreases as its volume and percentage of nanoparticle increases, while the velocity of the  $Al_2O_3$ -water nanofluid somewhat increases. Figure 5 shows that the thermal conductivity of the nanofluid increases with the concentration of nanoparticles, thickening the thermal boundary layer. This can be seen in the temperature profiles, which become increasingly apparent as the volume percentage increases (Figure 1). Because copper has superior electrical and thermal conductivity, the Cu-water nanofluid exhibits a broader thermal spread than the  $AlO_3$ -water nanofluid. Although the concentration profile of  $AlO_3$ -water generally follows a similar trend to that of Cu-water, Figure 6 shows that it falls as nanoparticle concentration increases.

Figure 7 shows how the parameter for heat generation  $Q$  affects the thermal behavior of both nanofluids. Cu-water nanofluids achieve greater temperature levels than  $Al_2O_3$ -water nanofluids, and both fluids exhibit higher temperature profiles as  $Q$  increases. Heat production increases cause the thermal boundary layer to thicken and thermal conductivity to increase.



Viscosity dissipation parameter ( $Ec$ ) effects on temperature profile are assessed in Figure 8. The temperature in both nanofluids rises as  $Ec$  does, suggesting that viscous heating plays a major role in energy distribution. Due to their greater thermal reactivity, Cu-water nanofluids exhibit a more noticeable increase.

The effect that the thermal radiation parameter ( $R$ ) has on the nanofluids is seen in Figure 9. For both Cu-water and  $AlO_3$ -water nanofluids, the temperature profiles grow with increasing  $R$ . Once again, the Cu-water nanofluid exhibits a more significant temperature increase. In order to promote energy dissipation from the fluid domain, the radiation thickens the thermal boundary layer, which is linked to higher Rosseland numbers and improves radiative heat transfer.

Figure 10 looks at how solute concentration profiles are affected by the Schmidt number  $Sc$ . Lower solute concentrations in both nanofluids are correlated with higher  $Sc$  values. Nonetheless, the Cu-water nanofluid's concentration profile is still somewhat more noticeable than the  $AlO_3$ -water nanofluid's.

Lastly, the effects of the chemical reaction rate parameter  $Kr$  and the Soret number  $Sr$  on solute concentration are discussed in Figures 11 and 12. The findings demonstrate that for both nanofluids, the solutal boundary layer thickens due to the Soret effect (thermo-diffusion). However, Cu-water nanofluid exhibits a greater enhancement in concentration profile with rising  $Sr$  compared to  $Al_2O_3$ -water. Interestingly, variations in the chemical reaction parameter  $Kr$  do not significantly alter the velocity or temperature distributions of either nanofluid, though noticeable differences in solutal concentration profiles between the two nanofluids are evident in Figure 11.

## 6. Conclusion

We study how a magnetic field affects the intricate behavior of nanofluids traveling across a stretched surface. Heat generation, chemical reactions, thermal radiation, and viscous dissipation are all examined in this work in relation to steady magnetohydrodynamic (MHD) flow of the boundary layer through a porous media.

- Under the identical conditions, the velocity of the  $AlO_3$ -water nanofluid increases as the volume and percentage of nanoparticle increases, but the velocity of the Cu-water nanofluid falls.
- For both kinds of nanofluids, decreasing velocity profiles are the result of increasing the permeability of the porous medium and the strength of the magnetic field.
- The temperature profiles of both nanofluids increase as the volume fraction of nanoparticles increases. Their concentration profiles, however, display distinct patterns: the Cu-water nanofluid shows the opposite tendency, whereas the  $Al_2O_3$ -water nanofluid shows a decrease in concentration with an increase in volume fraction.
- Increasing the rate of chemical reaction parameter and Schmidt number causes the concentration profiles of both nanofluids to fall. Higher Soret number values, on the other hand, improve the concentration profile.
- The thermal boundary layer thins more slowly when nanoparticles are present, heat radiation, porous medium effects, and viscous dissipation all occur.

Generally, the boundary layers of temperature, concentration, and velocity close to the stretch surfaces are thicker in  $AlO_3$ -water nanofluids than in Cu-water nanofluids.



Received: 16-09-2025

Revised: 05-10-2025

Accepted: 02-11-2025

Physical properties	Base fluid (H <sub>2</sub> O)	Copper (Cu)	Alumina (Al <sub>2</sub> O <sub>3</sub> )
$C_p$ (J/kgK)	4179	385	765
$\rho$ (Kg/m <sup>3</sup> )	997.1	8933	3970
$k$ (W/mK)	0.613	401	40

**Table-1: Thermal physical properties.**

Table 2. Comparison of the SRM solutions for  $f''(0)$ ,  $-\theta'(0)$ , and  $-\phi'(0)$  for different values of  $Sr, Sc, Q$  and  $Kr \cdot \phi = 0.1, E_c = 1, M = 0.5, Sc = 1, Q = 0.02, Pr = 7, K_1 = 1, Kr = 0.08, Sr = 0.2$ .

Cu +water			Al <sub>2</sub> O <sub>3</sub> + water			
	$\phi = 0.1, E_c = 1$		$R = 1.5, Pr = 7$		$K_1 = 1.25, M = 0.5$	
$Sr$	$f''(0)$	$-\theta'(0)$	$-\phi'(0)$	$f''(0)$	$-\theta'(0)$	$-\phi'(0)$
0.0	1.67923	0.264822	1.205443	1.543656	0.387837	1.234462
0.1	1.67923	0.264822	1.206502	1.543656	0.387837	1.226048
0.3	1.67923	0.264822	1.208618	1.543656	0.387837	1.209225
0.4	1.67923	0.264822	1.209677	1.543656	0.387837	1.200809
Sc						
0.6	1.67923	0.264822	1.20756	1.543656	0.387837	1.217637
0.7	1.67923	0.264822	1.578602	1.543656	0.387837	1.591183
0.8	1.67923	0.264822	1.89231	1.543656	0.387837	1.906038
0.9	1.67923	0.264822	2.168352	1.543656	0.387837	2.182708
Kr						
0.6	1.67923	0.264822	1.142691	1.543656	0.387837	1.158075
0.7	1.67923	0.264822	1.221807	1.543656	0.387837	1.230985
0.8	1.67923	0.264822	1.441995	1.543656	0.387837	1.442644
0.9	1.67923	0.264822	1.646539	1.543656	0.387837	1.643275



Received: 16-09-2025

Revised: 05-10-2025

Accepted: 02-11-2025

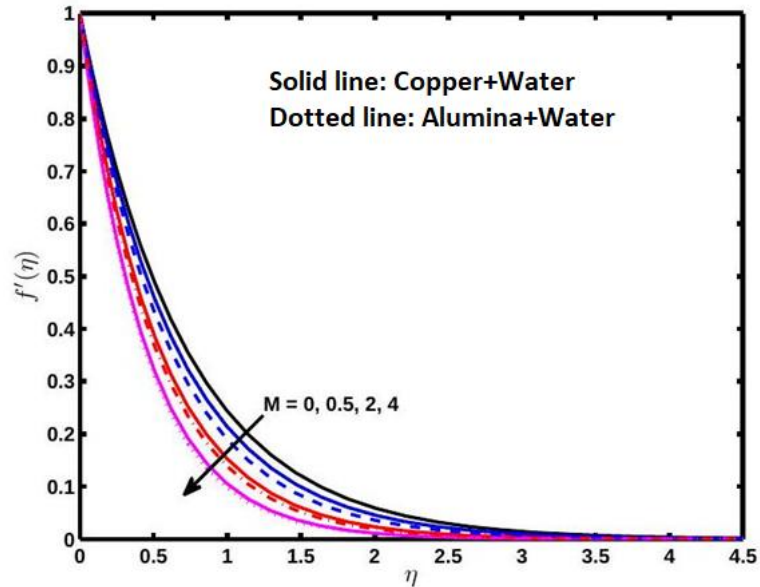


Figure 2. The magnetic parameter ( $M$ )'s effect on the fluid's velocity distribution.

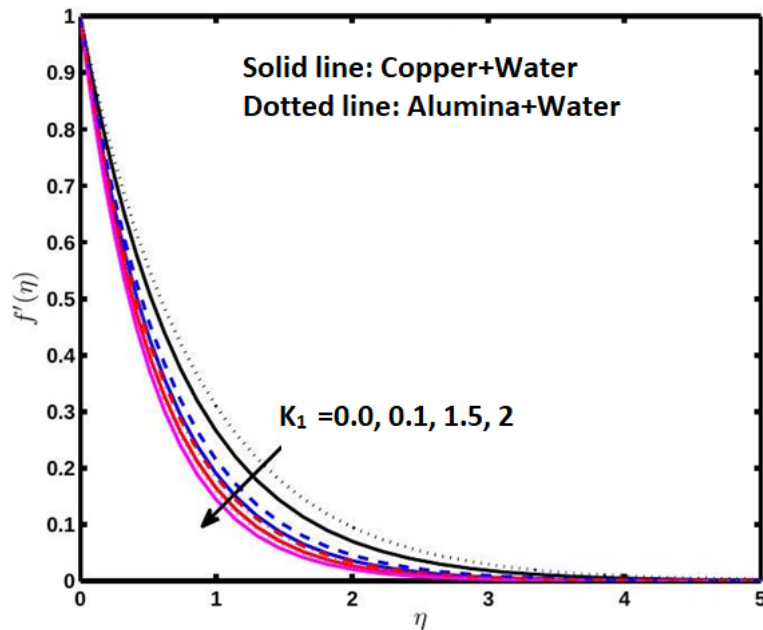


Figure 3. The porous medium parameter  $K_1$ 's influence on the velocity distribution.



Received: 16-09-2025

Revised: 05-10-2025

Accepted: 02-11-2025

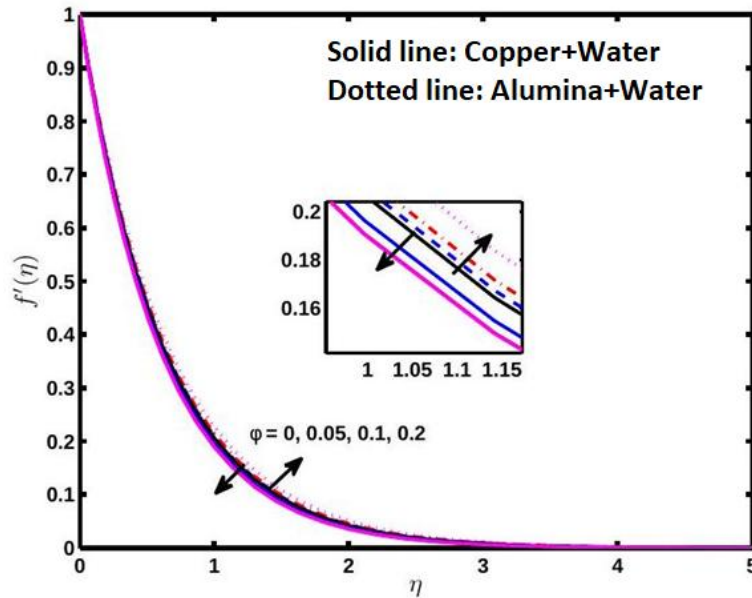


Figure 4. The impact of varying nanoparticle volume fractions ( $\phi$ ) on the velocity distribution.

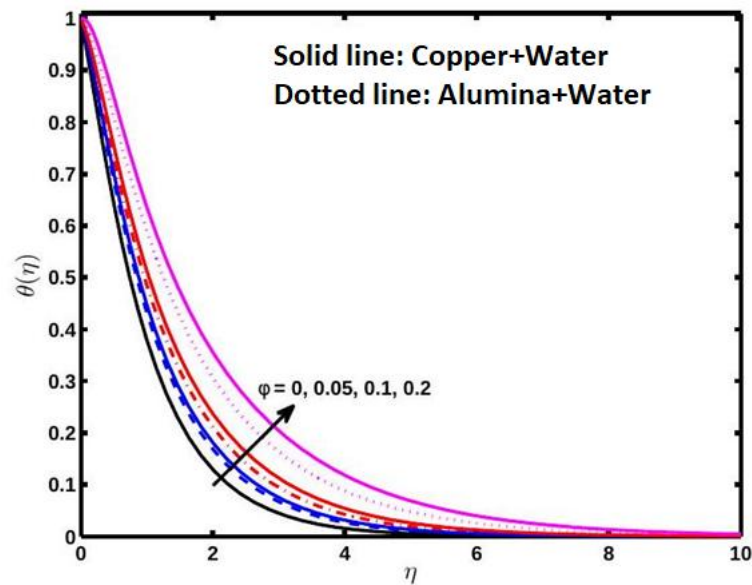


Figure 5. The impact of varying nanoparticle volume fractions ( $\phi$ ) on the temperature profiles.



Received: 16-09-2025

Revised: 05-10-2025

Accepted: 02-11-2025

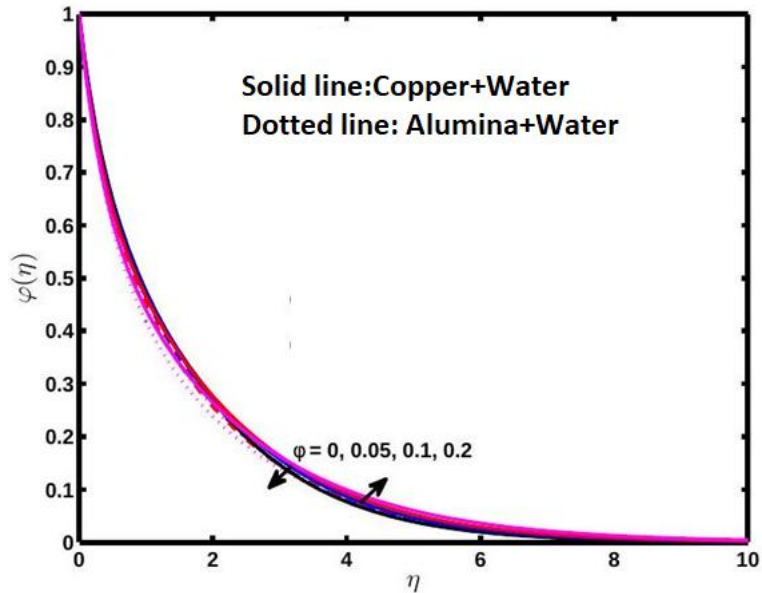


Figure 6. The effect of different volume fraction ( $\phi$ ) values on concentration profiles.

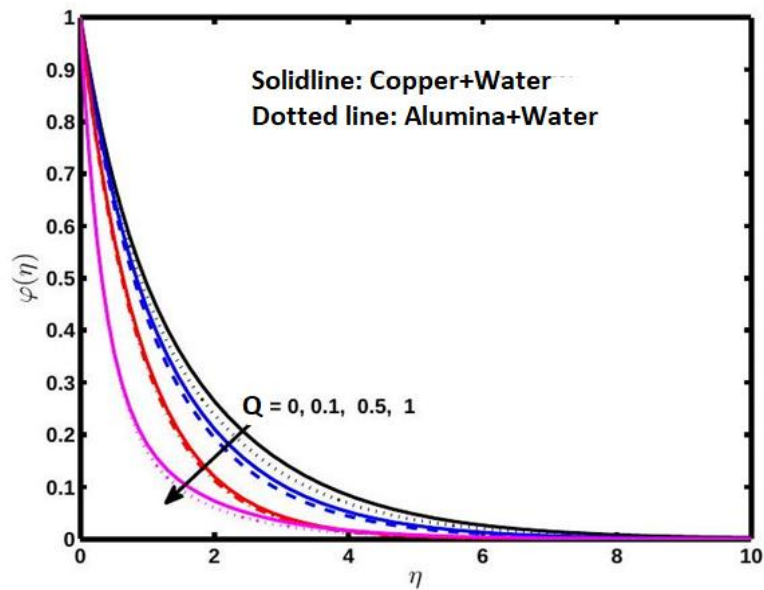


Figure 7. The impact of the heat generation parameter ( $Q$ ) on the temperature profiles.



Received: 16-09-2025

Revised: 05-10-2025

Accepted: 02-11-2025

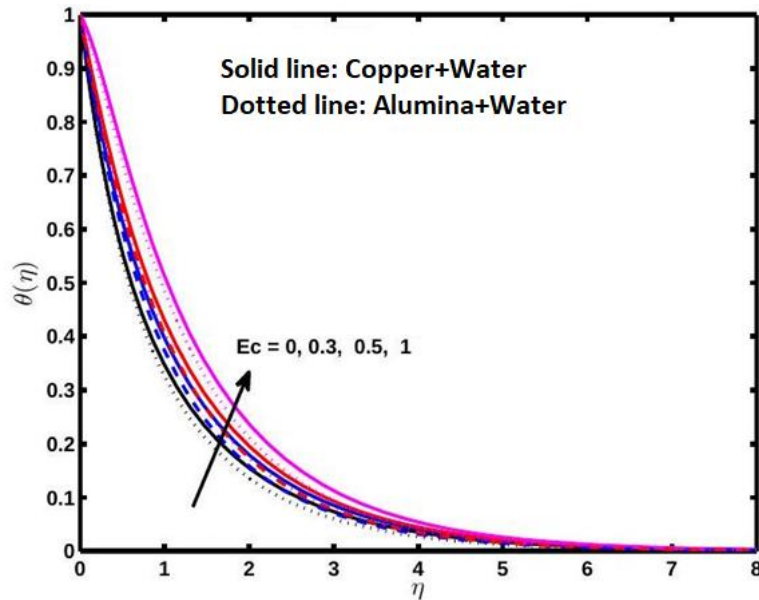


Figure 8. The impact of the viscous dissipation parameter ( $Ec$ ) on the temperature profiles.

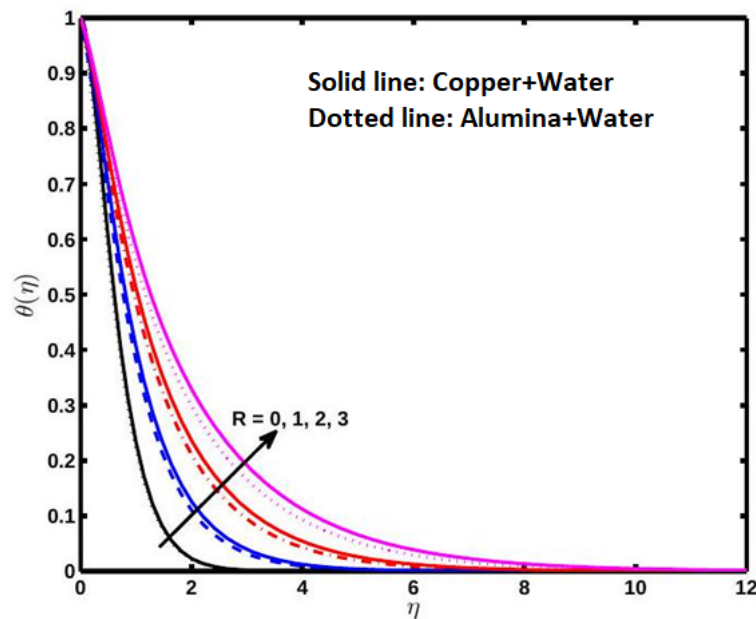


Figure 9. The impact of the thermal radiation parameter ( $R$ ) on the temperature profiles.



Received: 16-09-2025

Revised: 05-10-2025

Accepted: 02-11-2025

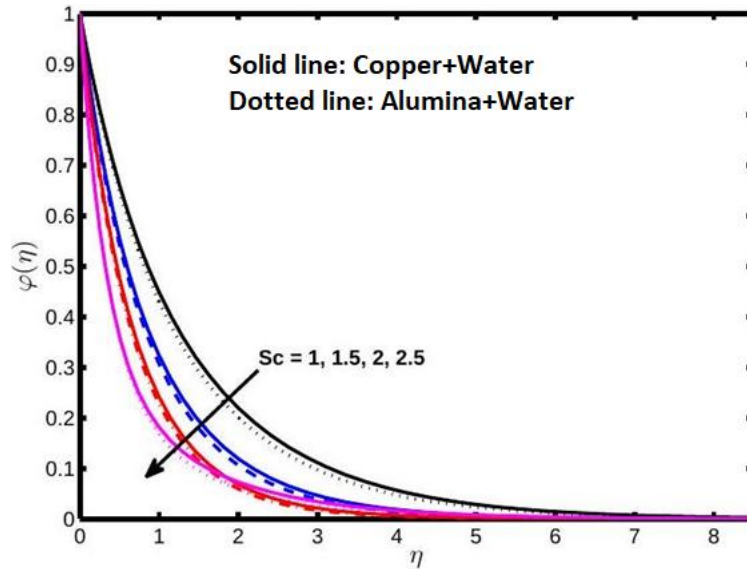


Figure 10. The impact of the Schmidt number( $Sc$ ) on the concentration profiles.

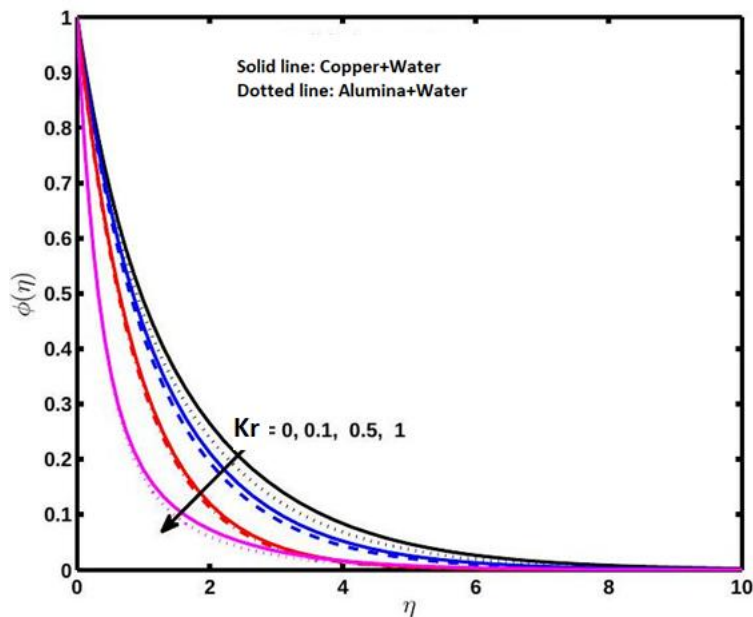


Figure 11. Effect of the chemical reaction parameter  $Kr$  on the concentration profiles.



Received: 16-09-2025

Revised: 05-10-2025

Accepted: 02-11-2025

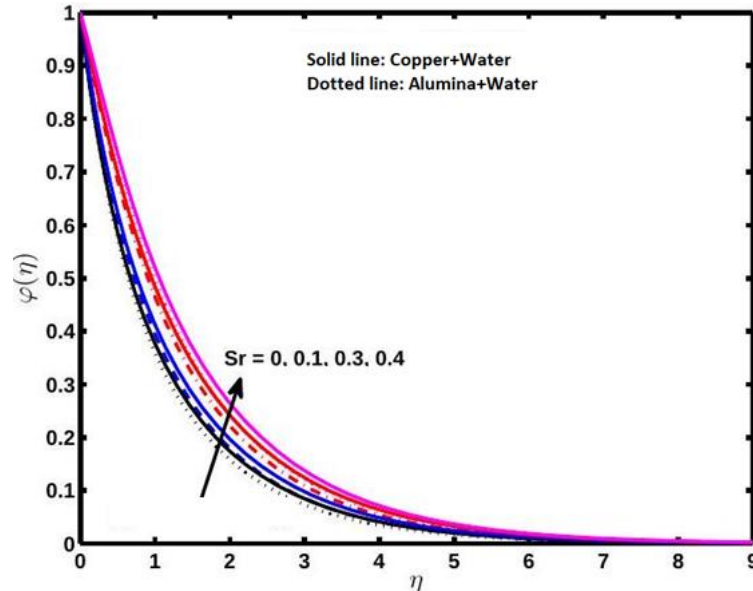


Figure 12. Effect of the Soret number  $Sr$  on concentration profiles.

## References

1. Crane, L.J. (1970): *Flow past a stretching plate*, ZAMP.-Angew Math. Phys, vol.21, pp.645 - 647. <https://doi.org/10.1007/BF01587695>
2. Khan, W.A. and Pop, I. (2010): *Boundary layer flow of a nanofluid past a stretching sheet.*- International Journal of Heat and Mass Transfer, vol.53, pp.2477 - 2483. <https://doi.org/10.1016/j.ijheatmasstransfer.2010.01.032>
3. Abd El-Aziz, M. (2007): *Thermal-diffusion and diffusion-thermo effects on combined heat and mass transfer by hydromagnetic three-dimensional free convection over a permeable stretching surface with radiation.*- Physics Letters, vol.372, No.3, pp.263-272. <https://doi.org/10.1016/j.physleta.2007.07.015>
4. Hady, F.M., Ibrahim, F.S., Abdel-Gaied, S.M. and Mohamed Eid, R. (2012): *Radiation effect on viscous flow of a nanofluid and heat transfer over a nonlinearly stretching sheet.*- Nanoscale Res. Lett vol.7, 229. <https://doi.org/10.1186/1556-276X-7-229>
5. Bachok, N., Ishak, A. and Pop, I. (2012): *Unsteady boundary-layer flow and heat transfer of a nanofluid over a permeable stretching/shrinking sheet*, International Journal of Heat and Mass Transfer, vol. 55, pp.2102 - 2109. <https://doi.org/10.1016/j.ijheatmasstransfer.2011.12.013>
6. Rohni, A.M., Ahmad, A.S. and Ismail, Md I. and Pop, I. (2013): *Flow and heat transfer over an unsteady shrinking sheet with suction in a nanofluid using Buongiorno's model.*- International Communications in Heat and Mass Transfer vol.43, pp.75 - 80. <https://doi.org/10.1016/j.icheatmasstransfer.2013.02.001>
7. Buongiorno, J., (2006): *Convective transport in nanofluids.*- ASME Journal of Heat Transfer vol.128, pp.240 - 250. <https://doi.org/10.1115/1.2150834>
8. Sandhya, A., Reddy, G. R., & Deekshitulu, G. V. S. R. (2020): *Heat and mass transfer effects on MHD flow past an inclined porous plate in the presence of chemical reaction.*- International Journal of Applied Mechanics and Engineering, vol.25,No.3,pp.86-102.<https://doi.org/10.2478/ijame-2020-0036>



Received: 16-09-2025

Revised: 05-10-2025

Accepted: 02-11-2025

9. Murthy, P.V. and Singh, P. (1997): *Effect of viscous dissipation on a non-Darcy natural convection regime.*- International Journal of Heat and Mass Transfer vol.40, pp.1251 - 1260. [https://doi.org/10.1016/S0017-9310\(96\)00181-0](https://doi.org/10.1016/S0017-9310(96)00181-0)
10. Motsa, S.S.(2013): *A New spectral relaxation method for similarity variable nonlinear boundary layer flow systems.*- Chemical Engineering Communications, vol.16, pp.23 - 57.
11. Gladys, T., & Reddy, G. R. (2022): *Contributions of variable viscosity and thermal conductivity on the dynamics of non-Newtonian nanofluids flow past an accelerating vertical plate.*- Partial Differential Equations in Applied Mathematics, vol.5, 100264. <https://doi.org/10.1016/j.padiff.2022.100264>
12. Vijaya, K., & Reddy, G. V. R. (2019): *Magnetohydrodynamic Casson fluid flow over a vertical porous plate in the presence of radiation, solet and chemical reaction effects.*- Journal of Nanofluids, vol.8, No.6, pp.1240-1248.
13. Oztop, H.F. and Abu-Nada, E. (2008): *Numerical study of natural convection in partially heated rectangular enclosures filled with nanofluids.*- International Journal of Heat and Fluid Flow vol.29, pp.1326 - 1336. <https://doi.org/10.1016/j.ijheatfluidflow.2008.04.009>
14. Brinkman, H.C.(1952): *The viscosity of concentrated suspensions and solution.*- Journal of Chemical Physics, vol.20, pp.571-581. <https://doi.org/10.1063/1.1700493>
15. J.C., Maxwell Garnett (1904): *Colours in metal glasses and in metallic films.*- Philosophical Transactions of the Royal Society of London, vol.203, pp.385-420. <https://doi.org/10.1098/rsta.1904.0024>
16. Abu-Nada , E.(2008): *Application of nanofluids for heat transfer enhancement of separated flows encountered in a backward facing step.*- International Journal of Heat and Fluid Flow, vol.29, pp.242-249. <https://doi.org/10.1016/j.ijheatfluidflow.2007.07.001>
17. Hamad, M.A.A. (2011): *Analytical solution of natural convection flow of a nanofluid over a linearly stretching sheet in the presence of magnetic field.*- International Communications in Heat and Mass Transfer, vol.38, pp.487 - 492. <https://doi.org/10.1016/j.icheatmasstransfer.2010.12.042>
18. Kameswaran, P.K., Narayana, M., Sibanda, P. and Murthy, P.V. (2012): *Hydromagnetic nanofluid flow due to a stretching or shrinking sheet with viscous dissipation and chemical reaction effects.*- International Journal of Heat and Mass Transfer vol.55, pp.7587 - 7595. <https://doi.org/10.1016/j.ijheatmasstransfer.2012.07.065>
19. Grubka, L.G. and Bobba, K.M. (1985): *Heat transfer characteristics of a continuous stretching surface with variable temperature.*- The ASME Journal of Heat Transfer vol.107, pp.248 - 250. <https://doi.org/10.1115/1.3247387>
20. Rafique, K., Mahmood, Z., & Khan, U. (2023): *Mathematical analysis of MHD hybrid nanofluid flow with variable viscosity and slip conditions over a stretching surface.*- Materials Today Communications, vol.36, 106692.
21. Nasir, S., Alghamdi, W., Gul, T., Ali, I., Sirisubtawee, S., & Aamir, A. (2023): *Comparative analysis of the hydrothermal features of TiO<sub>2</sub> water and ethylene glycol-based nanofluid transportation over a radially stretchable disk.*- Numerical Heat Transfer, Part B: Fundamentals, vol.83(5), pp.276-291.
22. P.M. Patil, B. Goudar, E. Momoniat(2023): *Magnetized Bioconvective micropolar nanofluid flow over a wedge in the presence of oxytactic microorganisms.*- Case Stud. Therm. Eng., Vol.49 103284, <https://doi.org/10.1016/j.csite.2023.103284>
23. S. Kumar Rawat, M. Yaseen, U. Khan, M. Kumar, A. Abdulrahman, S.M. Eldin, S. Elattar, A.M. Abed, A.M. Galal (2023): *Insight into the significance of nanoparticle aggregation and non-uniform heat source/sink on titania-ethylene glycol nanofluid flow over a wedge.* - Arab. J. Chem. Vol.16 104809, <https://doi.org/10.1016/j.ijheatmasstransfer.2012.07.065>



# Power System Technology

ISSN:1000-3673

*Received: 16-09-2025*

*Revised: 05-10-2025*

*Accepted: 02-11-2025*

24. J.C. Umavathi(2022): *Electrically conducting micropolar nanofluid with heat source/sink over a wedge: ion and hall currents.- J. Magn. Magn. Mater. Vol.559 169548, <https://doi.org/10.1016/j.jmmm.2022.169548>.*
25. K. Veera Reddy, D.Saidi Reddy, M.Anjaneyulu, N.Raju., "Electromagnetic and chemical reactions of unsteady viscoelastic flow of MHD Walter's-B through vertical porous plates." *Heat Transfer (2025), vol 54(3), 2345-2353. <https://doi.org/10.1002/htj.23292>*